JOURNAL OF MATERIALS SCIENCE **34** (1999) 1293–1300

Formation of ZnO/metal composites by rapid oxidation of Zn melts

D.-W. YUAN*, S. G. SONG†, R.-F. YAN, E. R. RYBA, G. SIMKOVICH
Department of Materials Science and Engineering, Pennsylvania State University, University Park, Pennsylvania 16802, USA

A novel ZnO-based composite material is fabricated by oxidation of Zn alloy melts, in which outward growth of the reaction products and rapid reaction kinetics are observed. Additions of Na and Bi to the Zn melts are found to be essential to increase the matrix growth rate to a practical level. Optimum reaction rates are observed for Zn-3Na-5Bi alloys oxidized at temperatures between 450 and 550 °C in pure oxygen. Processing parameters, such as alloy composition and oxygen activity, also have a profound impact on the resulting microstructure and reaction kinetics. The evidences supported that the continuous outward growth of the matrix is achieved via modification of the ZnO defect structure and partial wetting of the growing oxide by the melts.

1. Introduction

Rapid oxidation of liquid metals and alloys has to be avoided in melt processing because it leads to material losses and alloy composition changes as a result of preferential oxidation. However, the Dimox^{TM} process [1–4] has demonstrated that an unusually rapid oxidation reaction of a melt can be used to fabricate ceramic-based composites. The reaction products grow outward due to capillary rise of liquid metal to the reaction front through channels in the oxidation products. The final material is a three-dimensional interconnected ceramic network with some residual metal. Reinforcing materials in the form of particulates, platelets, whiskers and fibers can be placed adjacent to the metal so that the matrix grows through the materials without displacing the filler. This process overcomes the problems of densification shrinkage, and near-net-shape products can be formed. Also, strength and toughness are significantly enhanced over those observed in monolithic ceramics with the same matrix [5, 6].

To date, the advances of this technology have been focused primarily on Al_2O_3/Al and AlN/Al composites [7–9]. Processing variables play important roles on the growth rate and microstructure of the resulting materials. In particular, alloy composition, reaction temperature, and oxygen activity were found to be most critical [10, 11]. These indicate the flexibility and potential versatility of this technique. However, applicability of the Dimox^{TM} type process to other alloy systems has not been thoroughly examined. In this study, zinc was selected as the base metal because of its low melting point (419.5 °C) and slow oxidation kinetics at elevated temperatures [12]. Efforts were made to understand how the reaction rate can be increased and what mechanisms are operational where outward growth of the reaction products is promoted.

2. Experimental procedures

The alloys used in this investigation were made by melting charges of 99.94 % pure zinc with chemically pure grade alloying elements. The metals were assembled according to the stoichiometry chosen, in atomic percent (at %), and placed in Al_2O_3 crucibles. Al_2O_3 was selected for the container material because of its high chemical stability. The crucibles were then encapsulated in Pyrex glass tubing which had been evacuated and backfilled with argon to prevent oxidation. All the thermal treatments were performed in a muffle furnace, which had been calibrated prior to use. The Pyrex capsules were shaken periodically to ensure complete mixing of the Zn and the alloying constituents. The melts were furnace cooled. Alloy compositions are given in atomic percent throughout this paper unless otherwise designated.

Thermogravimetric analysis was used to measure weight changes as a function of time in oxidizing environments. The samples were suspended with a platinum wire from an arm of a Cahn 1000 automatic recording balance in a quartz reaction tube. The samples were heated to the selected temperatures from room temperature at a rate of 5 °C/min. Kinetics measurements were made in pure oxygen or in oxygen atmospheres diluted with argon. The gas flow rate dependence of the growth rate was determined to assure that measurements were made in a regime insensitive to flow rate. The nominal

* *Present address:* Concurrent Technologies Corporation, Johnstown, PA 15904.
† *Present address:* United Technologies Research Center, East Hartford, CT 06108.

cross-sectional area of the Al_2O_3 crucibles, 2.1 cm^2, was used as the materials growth surface area for the calculation of reaction rates.

The resulting ZnO based materials were prepared according to standard metallographic procedures and examined by a light microscope. A Scintag powder X-ray diffractometer (XRD) was employed for the phase identification of the bulk materials. The specimens were scanned at 3° (2θ) per minute using CuK_α radiation. In addition, the reaction products of Zn alloys were examined using a Phillips 420T analytical transmission electron microscopy (TEM) at operation voltage of 120 kV.

Wetting experiments were carried out in a horizontal tube furnace fitted with an observation window through which one could photograph a sessile drop. Pure ZnO disks, sintered at 1300 °C for 2 h, were used as the substrates. The samples were assembled and outgassed in the furnace with cleansed argon for 4 h. The desired atmosphere was then established, and the furnace ramped to temperature. Photographs of the sessile drops were taken at 5 min intervals up to 30 min.

3. Results and discussion

3.1. Pure Zinc and binary Zn alloys

To better understand the oxidation behavior of zinc in its molten state, kinetics studies were first carried out. Fig. 1a shows the weight gain per unit area as a function of time at temperatures ranging from 600 to 900 °C. Linear relationships between the square of weight gain per unit area and time, indicative of parabolic reaction kinetics, were observed when pure zinc is oxidized at temperatures up to 700 °C (Fig. 1b). At 800 and 900 °C, the high vapor pressure of the zinc may have resulted in material losses and, hence, the non-parabolic oxidation kinetics. During oxidation, a parabolic growth rate generally indicates that the growth of the oxide scale is controlled by counterdiffusion of ionic defects and electrons arising from non-stoichiometry. As a result, a composition gradient exists between the metal-scale and the scale-oxidant boundaries when local equilibrium is established. It has been shown that zinc oxide is an *n*-type semiconductor with zinc interstitials compensated by the quasi-free electrons as follows [13].

$$\mathrm{ZnO} = \mathrm{Zn}_i^{\cdot\cdot} + 2e' + \frac{1}{2}\mathrm{O}_2 \qquad (1)$$

Therefore, the oxidation of zinc in the molten state is considered to be controlled by the diffusion of defects associated with zinc interstitials in the growing solid ZnO.

To increase the oxidation rate of Zn, various alloying elements were added. It was found that most of the changes in oxidation rates observed are in accord with the Hauffe's valence rule for a cation-excess oxide (*n*-type) [14]. The introduction of a minor constituent of greater valence than Zn ions, such as aluminum, yttrium and niobium, decreases the oxidation rate of liquid Zn. Ions of the same valence, magnesium, have no significant effect on the overall oxidation rate. In contrast, the introduction of a minor amount of an element of lower valence, i.e., sodium and lithium, increases

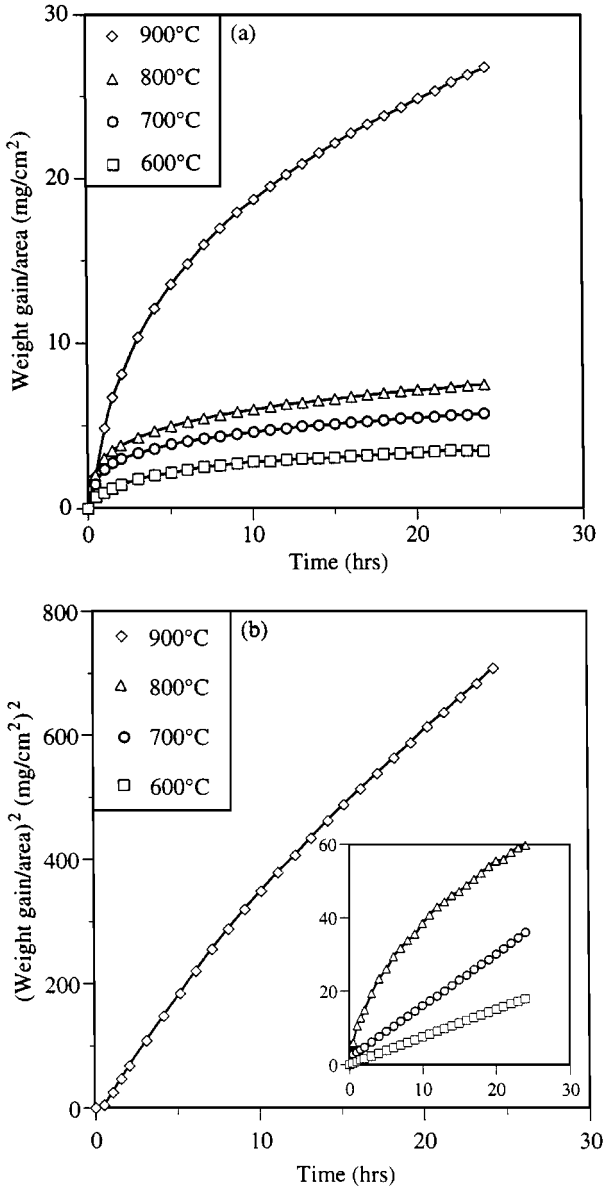

Figure 1 (a) Weight gain per area and (b) square of weight gain per area for pure Zn at different temperatures in 1 atm O_2.

the oxidation rate of Zn. Moreover, it was observed that Zn-Na alloys oxidized at a much faster rate than Zn-Li alloys. This finding can be related to the ionic size difference of the dopants, where Na^+ (1.02 Å) is much larger than both Li^+ (0.74 Å) and Zn^{2+} (0.75 Å). Therefore, the substitution of sodium ions in the ZnO structure dilates the structure locally. This expansion of the structure will then reduce the work required to squeeze a Zn ion from one site to a neighboring one [15]. As a result of lowered energy for diffusion, the diffusion rate of Zn ions increases in the Zn-Na alloys as well as the oxidation rate.

3.2. Ternary Zn-Na-Bi alloys

A third element was introduced into Zn alloys due to the failure of numerous binary alloys to react with oxygen in a rapid and progressing manner. The general considerations in the selection of such an addition are: (a) low melting point, which means the solidification temperature of the alloy prepared is most likely to be lower, and a greater temperature range can be tested;

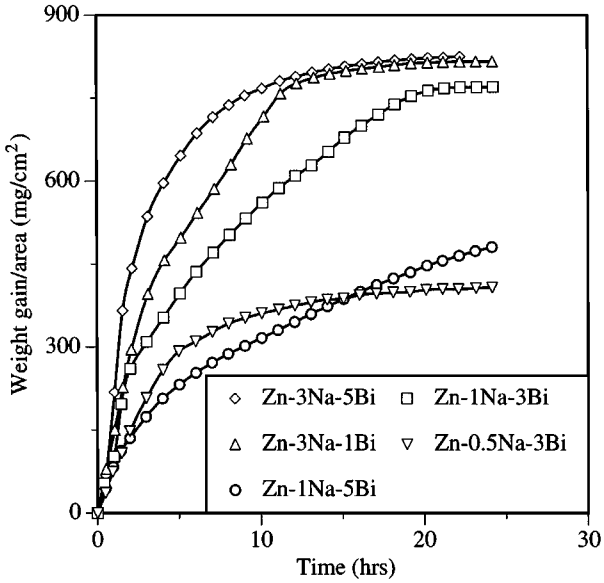

Figure 2 Weight changes for selected Zn-XNa-YBi ($X = 0.5$–3, $Y = 1$–5) alloys at 550 °C in 1 atm O_2.

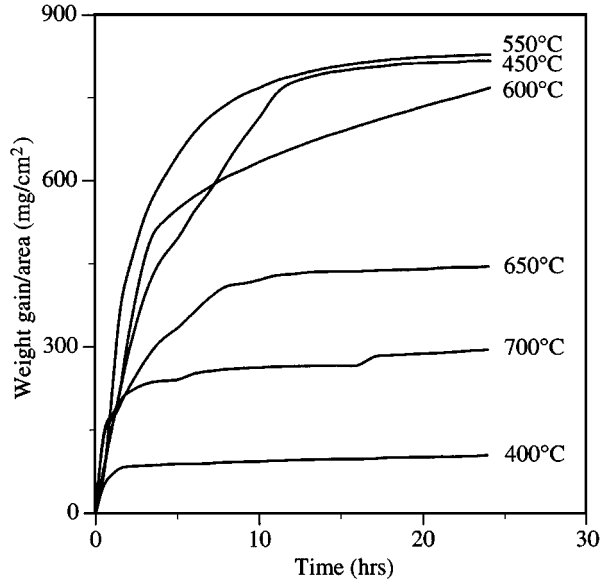

Figure 3 Weight changes for a Zn-3Na-5Bi alloy at various temperatures in 1 atm O_2.

(b) low surface tension, which facilitates the wetting of the oxide by the melts; and (c) lower oxygen affinity than zinc, which enables the alloying additions to remain soluble in the melts and consequently reinforce (a) and (b). Based on these selection criteria, bismuth is considered to be one of the leading candidates to fulfill the requirements. In this paper, further discussion is limited to the modification of binary Zn-Na alloys, which have shown the potential to achieve high reaction rates.

Oxidation kinetics for selected Zn-Na-Bi alloys of different dopant concentrations (0.5–3% Na, 1–5% Bi) at 550 °C in oxygen are shown in Fig. 2. These results show that changing the melt composition dramatically alters the reaction rate. Among the alloys, Zn-3Na-5Bi was observed to possess the fastest growth rate and the highest metal-to-oxide conversion ratio. Examination of the cross-section of the crucible and the oxide revealed a continuous outward growth of the reaction product and the presence of cavities at the bottom of the crucible. These are the two typical characteristics of the Dimox^{TM} type reaction. Similar growth behavior of the alloys has also been observed when melts were contained in ZrO_2 and MgO crucibles [16].

In addition to alloy composition, reaction temperature is expected to have a pronounced effect on the composite growth rate and microstructure. As shown in Fig. 3, the oxidation rates of the Zn-3Na-5Bi alloy are maximized at temperatures of 450–550 °C, at which more than 80% of the metals reacted to form oxide. Reactions become sluggish at temperatures higher than 700 °C or lower than 450 °C. Table I lists the initial linear growth rates of the alloys at various temperatures. For comparison, the growth rates for two binary alloys and pure Zn are also included.

3.3. Characterization of the ZnO/Zn composite

XRD analyses of the crushed reaction product of Zn-3Na-5Bi alloy at 550 °C show that ZnO is the predominant phase, and metallic Zn and Bi are the two minor constitutents in the composite. However, significant variations in intensity of selected peaks in the X-ray diffraction patterns are identified between sections of the specimens cut parallel and perpendicular to the growth direction. Table II lists the intensities for selected peaks. The intensities of the peaks are normalized to $I_{101} = 100$. The crushed composite powder exhibits peak intensities close to those expected for randomly oriented ZnO. For composite sections cut perpendicular to the growth direction, the intensities of the (hk0) type diffractions are significantly enhanced while the intensities from (00l) planes are decreased. The opposite is observed for sections cut parallel to the growth direction. These results indicate a preferred growth

TABLE I Average growth rates of various Zn alloys in O_2

Alloy	Reaction temperature (°C)	Growth rate (g/cm^2 s)
Zn	550	8.3×10^{-8}
Zn-5Bi	550	9.9×10^{-8}
Zn-3Na	550	4.4×10^{-6}
Zn-1Na-3Bi	550	2.5×10^{-5}
Zn-3Na-5Bi	650	2.2×10^{-5}
Zn-3Na-5Bi	550	4.2×10^{-5}
Zn-3Na-5Bi	450	3.2×10^{-5}

TABLE II Comparison of relative X-ray diffraction intensities for different ZnO materials

		ZnO composite		
Selected *hkl* for ZnO	Random orientation (PDF#36-1451)	Crushed	Section cut perpendicular to growth	Section cut parallel to growth
101	100	100	100	100
100	57	61	110	51
110	32	25	56	25
200	4	3	9	2
002	44	48	16	109
004	2	2	4	9

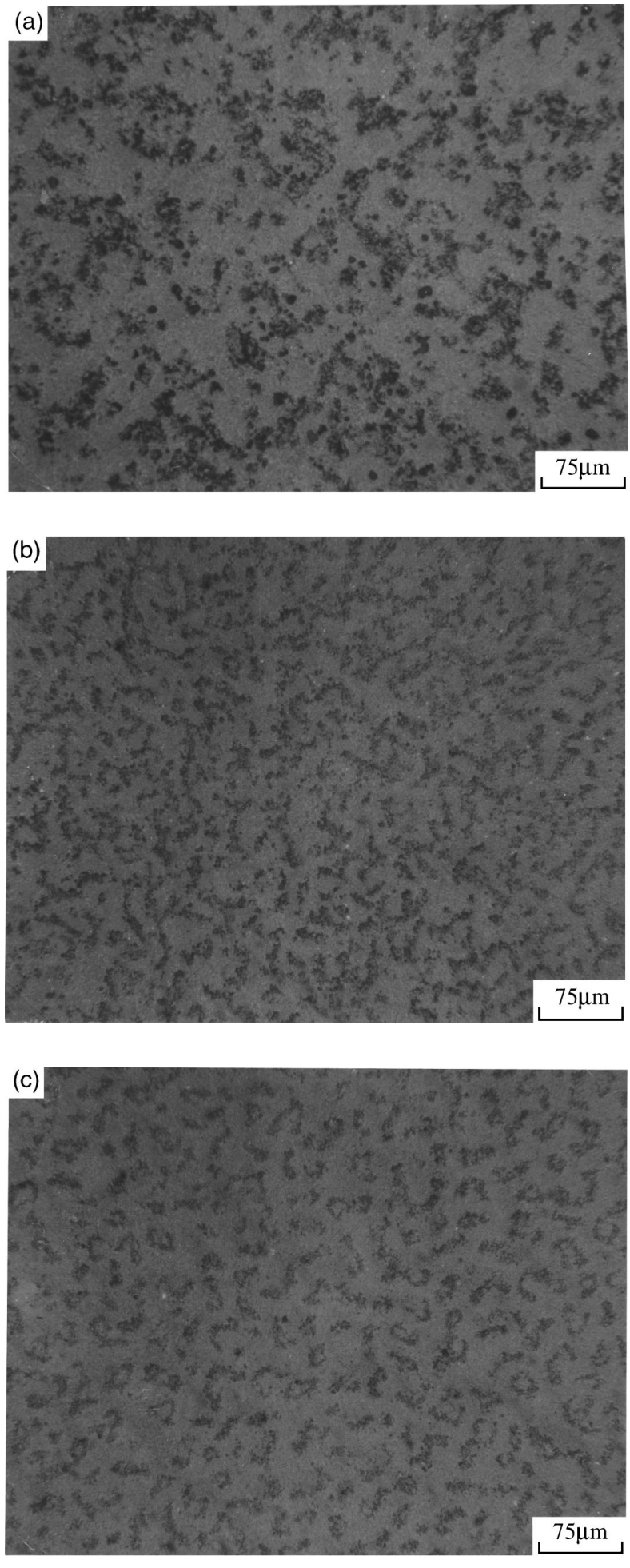

Figure 4 Optical micrographs of the polished surface of (a) Zn-3Na-5Bi, (b) Zn-1Na-3Bi and (c) Zn-3Na-1Bi alloys oxidized at 550 °C in O_2.

direction of the ZnO along ⟨100⟩ direction. No preferred orientation was detected for the metallic phases.

Fig. 4a shows an optical micrograph of a polished section of a composite material after oxidation of a Zn-3Na-5Bi alloy at 550 °C for 24 h. The structure consists of an interconnected ZnO matrix (light phase) and partially interconnected metallic phases (dark phase). As expected, alloy composition also has an impact on the composite microstructure. Fig. 4b shows an optical micrograph of the resulting oxide microstructure (top region) from a Zn-1Na-3Bi alloy. This alloy, of lower conversion ratio (i.e., Zn-1Na-3Bi), produces a microstructure containing a higher volume fraction of metals while the alloy of higher conversion ratio (i.e., Zn-3Na-5Bi) results in a microstructure of higher ceramic to metal ratio. In comparison, Fig. 4c shows the reaction products of a Zn-3Na-1Bi alloy oxidized at 550 °C in which the conversion ratio was observed to be comparable to the Zn-3Na-5Bi alloy (Fig. 2).

In addition, the effect of oxygen partial pressure on the composite growth rate of Zn-3Na-5Bi alloy was investigated. Fig. 5 shows that the oxidation rate decreases progressively as oxygen activity decreases. The growth rate at 550 °C is proportional to $P_{O_2}^{1/2}$, as illustrated in Fig. 6. Moreover, lower oxygen partial pressures were found to be responsible for smaller grain sizes of the metallic constituents in the resulting microstructure.

3.4. Growth mechanism of ZnO based composites

One factor that required amplification was whether it was necessary to use ternary Zn-Na-Bi alloys to retain rapid oxide growth. Table I includes the reaction kinetics for the binary system. The rates are drastically lower than that of the ternary alloys. In addition, visual examination of the reaction products of the binary alloys showed no outward growth, and the color of the oxide scale was gray instead of black, typical for the ZnO/metal body.

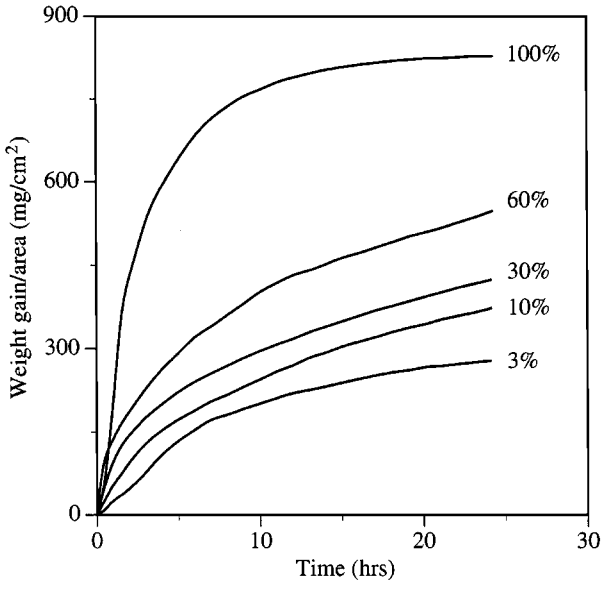

Figure 5 Weight changes for a Zn-3Na-5Bi alloy at 550 °C in various oxygen partial pressures.

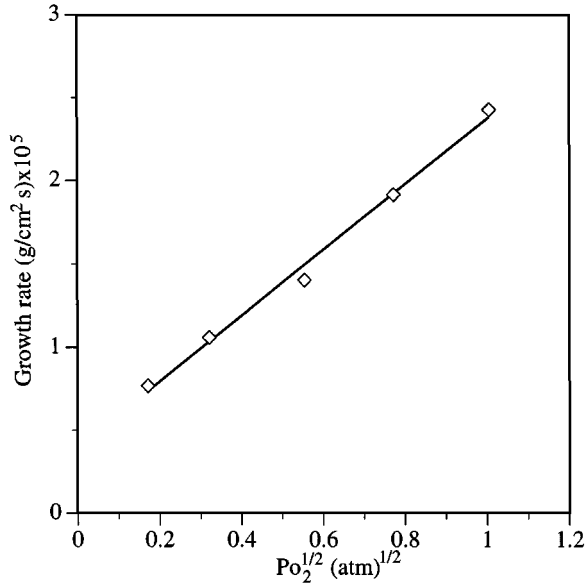

Figure 6 The rate constant for the oxidation of Zn-3Na-5Bi alloy at 550 °C as a function of the square root of oxygen pressure.

It becomes apparent that critical processing conditions have to be met in order to obtain rapid growth rate of the composite materials. Therefore, a satisfactory mechanism must address a number of unusual features of the oxidation process and the resulting materials:

(1) The oxidation reaction product is non-protective, in contrast to the normal behavior of a ZnO film. Further, the observed oxide formation rates are much higher than usual for alloys forming ZnO scales, and the growth occurs at a nearly constant rate in an outward direction.

(2) The reaction product typically contains both interconnected ZnO and partially interconnected Bi and Zn. ZnO matrix material grows preferentially along ⟨100⟩.

(3) The process occurs at rapid rates only over a certain range of temperatures. Above and below these temperatures, growth can be much slower.

(4) Changing the partial pressure of the oxidant can alter the kinetics and resulting microstructure. Also the growth rate exhibits an oxygen partial pressure dependence of $P_{O_2}^{1/2}$.

Observations in sessile drop experiments indicate that liquid Zn-Na-Bi alloys partially wet the ZnO/metal composite ($0 \approx 30°$) at 550 °C in purified argon. This suggests that the surface energy of the solid/vapor interface is greater than that of the solid/liquid interface according to the Young's equation [17].

$$\theta = \cos^{-1}\{(\gamma_{SV} - \gamma_{SL})/\gamma_{LV}\} \quad (2)$$

where γ is the surface energy and the subscripts S, L and V represent solid, liquid and vapor phases, respectively. In comparison, no wetting was observed (i.e., $\theta > 90°$) when a pure Zn droplet is rested on the same ceramic plate. Yeum *et al.* [18] reported that low-surface-tension components tend to concentrate on the surface layer and thus can sharply lower the surface energy of the melts.

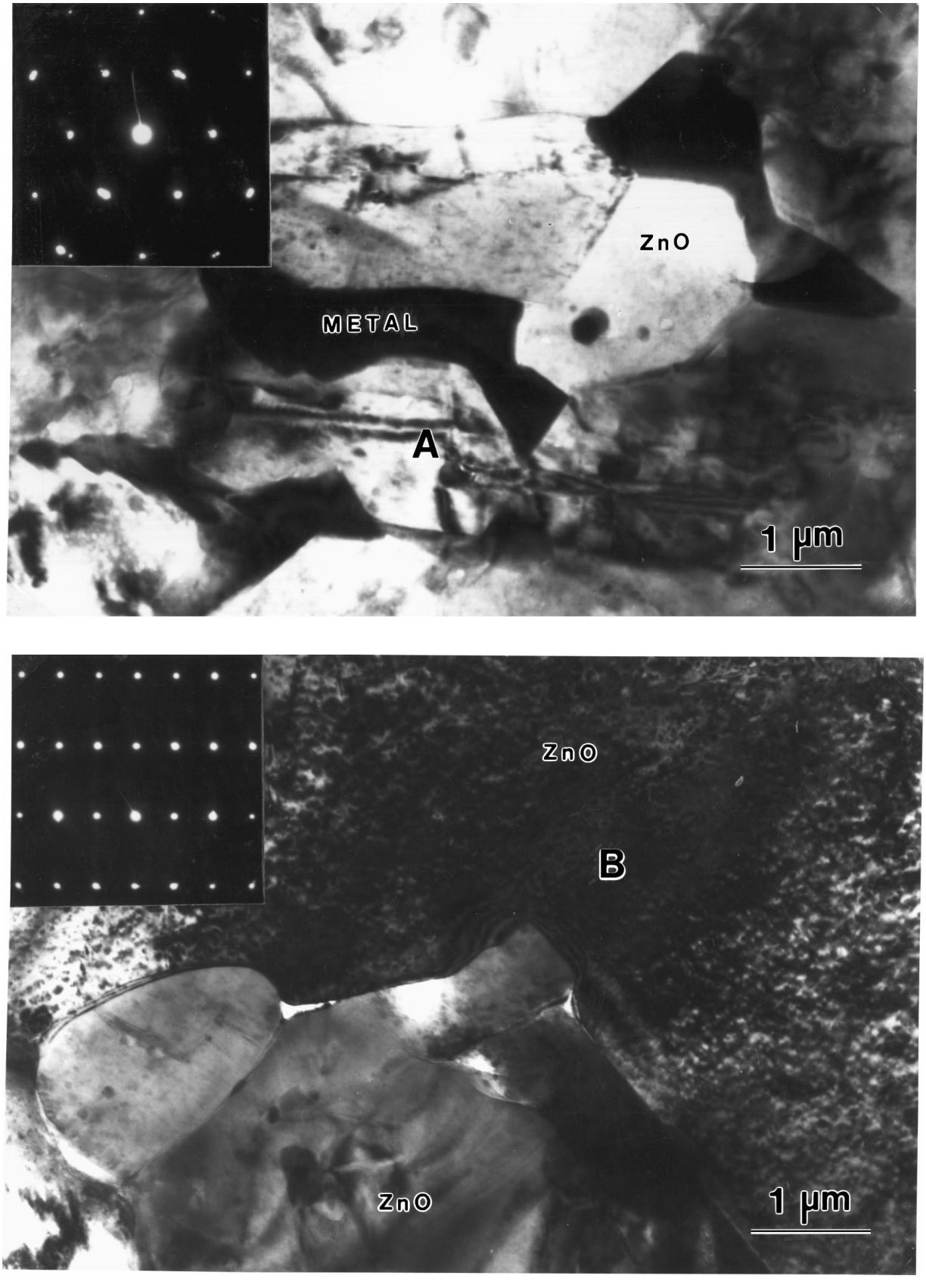

Figure 7 TEM bright field micrographs of the typical morphologies of ZnO and metals in the reaction products, from which a Zn-3Na-5Bi alloy is oxidized at 550 °C in oxygen.

On the contrary, the influence on the surface tension is insignificant when components of higher surface tension are added, because they are less concentrated on the surface layer than in the bulk. Liquid bismuth is known to have a lower surface tension (378 mNm^{-1} at 271 °C) than liquid zinc (782 mNm^{-1} at 420 °C) [19]. Therefore, additions of Bi to the melts can markedly decrease the surface tension and, consequently, facilitate the wetting of the ceramic by the liquid alloy. Liquid Na also has a low surface tension (191 mNm^{-1} at 98 °C).

However, its low Gibbs energy of formation, i.e., high oxygen affinity, makes it thermodynamically unstable in an oxidizing environment and thus ineffective in lowering the surface tension of the melts.

Figs 7a and b show two different TEM bright field images of the morphologies of the ZnO and metallic constituents where the specimen was prepared from a section of the reaction product perpendicular to the growth direction. In Fig. 7a several ZnO grains are surrounded by metallic phases. Selected area diffraction (SAD) patterns of the grain marked with "A" (inset in Fig. 7a) indicates that the [001] axis (*c*-axis) of the ZnO is nearly coincidental with the incident beam direction (composite growth direction). This is confirmed by the near hexagonal shape of the grain. In contrast, Fig. 7b shows a region where the ZnO grains are much larger than those in Fig. 7a. A SAD pattern of the ZnO grain "B" (inset in Fig. 7b) shows that the [100] axis is almost aligned with the outward growth direction of the alloy. These observations indicate that growth of ZnO grains along the [100] direction is much more pronounced than along the [001] direction. Similar conclusions are made based on the XRD analysis results; outward growth of ZnO in the composite structure mostly takes place along the crystallographic directions perpendicular to the basal planes. In addition, the metal constituents encircling the matrix phase (Fig. 7a) can be considered as channels that draw the melt to the reaction front. The fact that they were found to be associated with type "A" rather than type "B" ZnO grains suggests the liquid/solid interface energy of the former is lower than the latter.

By wetting the resulting oxidation product, the liquid alloy can penetrate along the grain boundaries of the solid oxide to the gas/oxide interface by capillary rise. The horizontal rising velocity of the ternary liquid alloy along a cylindrical channel can be estimated according to Washburn's equation [20], assuming a contact angle of 30°.

$$\frac{\mathrm{d}l}{\mathrm{d}t} = \frac{r}{\eta}\frac{\gamma}{4l}\cos\theta - \frac{\rho g r^2}{8\eta} \tag{3}$$

where l is the depth of penetration, t is time, r is the radius of the capillary, η is the viscosity of the liquid, γ is the surface tension of the liquid/vapor interface, θ is the contact angle, ρ is the density of the fluid, and g is the acceleration due to gravity. The velocity of the flow in a channel of radius 10 μm is approximately three orders of magnitude faster than the observed oxide growth rate (Fig. 8). In reality, the calculations would be much more complex if tortuous channels of varying radius are taken into considerations. However, the near-constant oxidation rates suggest that the mass transport of the melts along the microscopic channels in the oxide to the reaction front is sufficient.

As shown in Fig. 6, the linear growth rate at 550 °C is proportional to the square root of oxygen activity over the whole pressure range studied. No diffusion process through a compact semiconductor oxide, or gaseous diffusion through a porous oxide, can account for the square root of the pressure dependence. A possible reaction mechanism calls for the dissociation of the

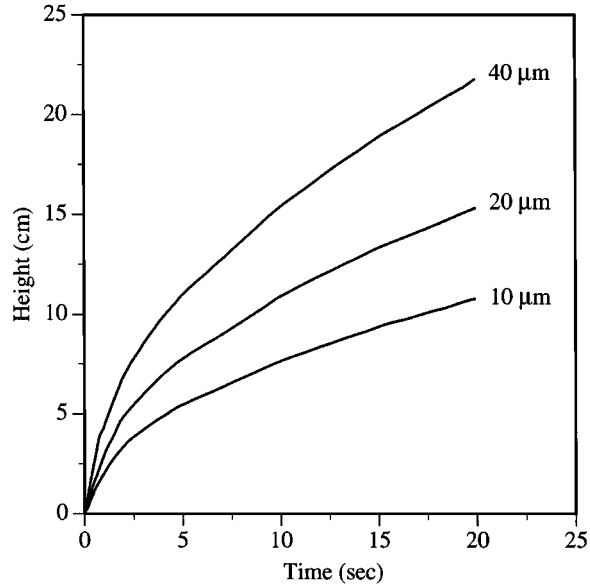

Figure 8 Calculated kinetics of a rising molten alloy in capillaries of different sizes.

oxygen molecules during the oxidation process [21]. It is assumed that the gas molecules initially become physically adsorbed on the interface and subsequently dissociate into oxygen atoms

$$O_2 = 2\underline{O} \tag{4}$$

The equilibrium constant is termed K and $Q = K^{1/2} \cdot P_{O_2}^{1/2}$. Subsequently, the $\underline{O}$ reacts to form ZnO. Combined with the oxygen activity dependence of the oxidation rate, it seems reasonable to propose that the dissociation of the adsorbed molecules to atoms is slower compared with the adsorption process, and is also slower compared with the incorporation of the separate atoms into the anion sites of the oxide.

It is concluded that oxidation of liquid Zn-Na-Bi alloys proceeds at the oxide/gas interface and the outward growth of the oxide matrix is sustained by the capillary rise of the melt to the reaction front. The schematic mechanism of the reaction is given in Fig. 9. The

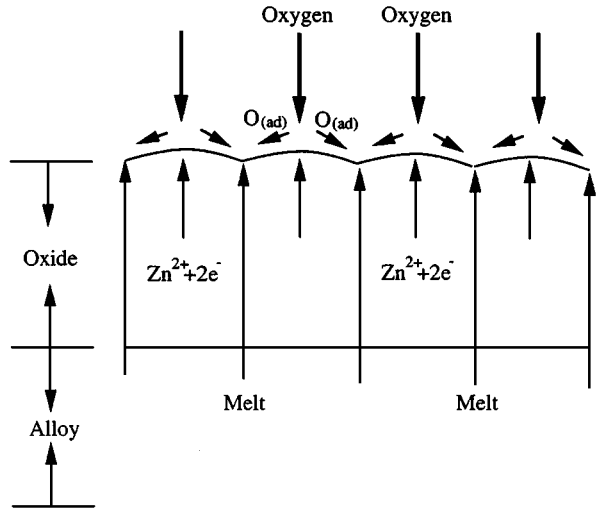

Figure 9 Schematic drawing for the mechanism of the formation of ZnO/metal composite materials.

lamellar structure represents the continuous and preferential growth of the ZnO network, and it can be seen that the ZnO provides a means of enhanced cation transport to the interface due to the doping of sodium. At the oxide interface, the low liquid/solid interface energy permits the penetration of the melt along the grain boundaries to the reaction front. From a reaction kinetics viewpoint, the mass transfer via grain boundaries would certainly outweigh the volume diffusion controlled growth process. As a result, a near-constant oxidation rate is observed. The observed changes in kinetics and microstructure with temperature can be understood if relative solid/liquid and solid/vapor interface energies vary as the temperature changes. At temperatures outside the 450–550 °C range, the wetting behavior between melt and reaction oxide can no longer sustain the rapid oxide growth. Eventually, a protective and impermeable oxide film forms and oxidation can only proceed at a parabolic rate. On the other hand, modification of the defect structure of ZnO by varying the alloy composition and oxygen partial pressure can also have an impact upon the relative values of interface energy. As a result, the kinetics and microstructure are varied accordingly.

4. Conclusions

For the oxidation behavior of binary Zn alloys, the effects of alloying additions are in general agreement with the prediction of Hauffe's rules. However, the increase in oxidation rate is limited and can not be sustained over extended times. The addition of Bi to the Zn-Na liquid alloys was essential for the initiation of a rapid and outward growth of the oxide matrix, an oxidation behavior analogous to the Dimox^{TM} type process. It has been shown that the oxidation rate is strongly dependent on the alloy composition, reaction temperature and oxygen activity. The fastest rate of 4.2×10^{-5} g/cm^2 s was observed for a Zn-3Na-5Bi alloy oxidized at 550 °C in pure oxygen, which is about 10^3 times greater than the rate of pure liquid zinc to solid zinc oxide at the same temperature. Moreover, the growth rate of Zn-Na-Bi alloys at 550 °C is proportional to the square root of oxygen partial pressure. This indicates that dissociation of adsorbed oxygen molecules is the rate-limiting step in the oxidation reaction.

The present findings indicate the applicability of the Dimox^{TM} type process to alloy systems other than A1 based materials. Several parallels in the materials processing between ZnO-based and Al_2O_3-based composites can be drawn:

(a) Rapid and near-constant growth rates of the matrix can only be achieved over fairly narrow temperature ranges and without excessive material loss due to evaporation.

(b) The resulting microstructure and properties can be tailored by altering the alloy composition and oxygen partial pressure.

(c) Modification of the defect structure of the base oxide by incorporating alivalent dopants of high oxygen affinities proves to be essential.

(d) Adequate wetting of the resulting oxides by the liquid alloys is essential to sustain an outward growth of the matrix.

References

1. S. NEWKIRK, A. W. URQUHART, H. R. ZWICKER and E. BREVAL, *J. Mater. Res.* **1** (1986) 81.
2. M. S. NEWKIRK, H. D. LESHER, D. R. WHITE, C. R. KENNEDY, A. W. URQUHART and T. D. CLAAR, *Ceram. Eng. Sci. Proc.* **8** (1987) 879.
3. Y.-M. CHIANG, J. S. HAGGERTY, R. P. MESSNER and C. DEMETRY, *Amer. Ceram. Soc. Bull.* **68** (1989) 420.
4. W. URQUHART, *Adv. Mater. Proc.* **140**(1) (1991) 25.
5. M. K. AGHAJANIAN, N. H. MACMILLAN, C. R. KENNEDY, S. J. LUSZCZ and R. ROY, *J. Mater. Sci.* **24** (1989) 658.
6. W.-P. TAI, T. WATARI and T. TORIKAI, *Amer. Ceram. Soc. Bull.* **76**(4) (1997) 86.
7. SINDEL, N. A. TRAVITZKY and N. CLAUSSEN, *J. Amer. Ceram. Soc.* **73**(9) (1990) 2615.
8. D. K. CREBER, S. D. POSTE, M. K. AGHAJANIAN and T. D. CLAAR, *Ceram. Eng. Sci. Proc.* **9**(7/8) (1988) 975.
9. D.-W. YUAN, V.-S. CHENGN, R.-F. YAN and G. SIMKOVICH, *Ceram. Sci. Eng. Proc.* **15**(4) (1994) 85.
10. A. S. NAGELBERG, *Mater. Res. Soc. Symp. Proc.* **155** (1989) 275.
11. A. S. NAGERBERG, *J. Mater. Res.* **7**(2) (1992) 265.
12. J. O. COPE, *Trans. Faraday Soc.* **57** (1961) 493.
13. G. HEILAND, E. MOLLOW and F. STOCKMANN, in "Solid State Physics," Vol. 8, edited by F. Seitz and D. Turnbull (Academic Press, New York, NY, 1959) p. 193.
14. K. HAUFFE and C. GENSCH, *Z. Physik. Chem.* **195** (1950) 116.
15. A. OVERHAUSER, *Phys. Rev.* **90** (1953) 393.
16. D.-W. YUAN and G. SIMKOVICH, *Ceram. Sci. Eng. Proc.* **13**(9) (1992) 581.
17. T. YOUNG, *Trans. Roy. Soc.* **95** (1805) 65.
18. K. S. YEUM, R. SPEISER and D. R. POIRIER, *Metall. Trans.* **20B** (1988) 693.
19. C. ALLEN, in "Liquid Metals: Chemistry and Physics," edited by S. Z. Beer (Marcel Dekker, New York, NY, 1972).
20. W. WASHBURN, *Phys. Rev.* **17** (1921) 273.
21. S. GLASSTONE, K. J. LAIDLER and H. EYRING, "The Theory of Rate Processes" (McGraw-Hill, New York, NY, 1941).

Received 16 October 1997
and accepted 4 November 1998